Estimation of ATMS Antenna Emission from Cold Space Observations

Hu Yang[1], Fuzhong Weng[2], and Kent Anderson[3]

1. University of Maryland
2. NOAA Center for Satellite Applications and Research
3. NGES

Submitted to ITSC-20 Proceedings

NOV 10, 2015

Abstract

The Advanced Technology Microwave Sounder (ATMS) onboard the Suomi National Polar-orbiting Partnership (NPP) satellite is a total power radiometer and scans across the track within a range of ±52.77° from nadir. It has 22 channels and measures the microwave radiation at either quasi-vertical or quasi–horizontal polarization from the Earth's atmosphere. ATMS scanning reflector is made of the beryllium coated with gold and can have an emission due to the surface roughness. An estimate of the reflector emissivity in the prelaunch phase was not explored. In this study, a new methodology is developed to assess the antenna emission from the ATMS pitch-over observations. It is found that the antenna emission is significant and dominates the scan angle dependent features in the ATMS antenna temperatures. Retrieved emissivity from K to G bands ranges from 0.002 to 0.006. Error model was also developed to assess the impact of antenna emissivity to calibration accuracy of antenna temperature products. Simulation results show that the calibration error are scene temperature dependent and can be as large as 2.5K for space view.

Keywords: Suomi NPP, ATMS, Antenna Emissivity

I. Introduction

On October 28, 2011, the Suomi National Polar-orbiting Partnership (NPP) satellite was successfully launched into a circular, near-polar, afternoon-configured (1:30 pm) orbit at an average altitude of 842 km above the Earth and an inclination angle of 98.7^{o} to the Equator. The Advanced Technology Microwave Sounder (ATMS) onboard the Suomi NPP satellite profiles atmospheric temperature and moisture in all-weather conditions, and supports continuing advances in numerical weather prediction (NWP) for improved short- to medium-range weather forecast skills, the ATMS instrument characteristics are listed in table 1. On February 20, 2012, ATMS on the Suomi NPP satellite was commanded to pitch over, scan the deep space and collect the 18-minutes of data with 96 of field of views (FOVs) along each scan. In principle, the brightness temperatures after calibration from the cold space should be uniform across the scan. In our previous studies, it has been found that the pitch maneuver data showed a scan-angle dependent radiometric bias with respect to the cold space background brightness temperature of 2.73 K. In particular, the biases at ATMS channels 1,2, and 16 are a sine-squared function of scan angle (smile shape) whereas the rest of channels are a cosine-squared function of scan angle (frown shape) (Weng and Yang et al., 2013). We also demonstrated that the near-field radiation from satellite platform and instrument itself may plays a critical role for the observed scan angle dependent bias. An empirical model is then established to explain the scan-angle dependent feature of ATMS measurement bias, with model parameters derived from the pitch-over maneuver data. The Quasi-V and Quasi-H polarized corrections are expressed as function of scan angle:

$$S_a^{Qv} = \beta_0 + \beta_1 sin^2\theta \tag{1a}$$

$$S_a^{QH} = \beta_0 + \beta_1 cos^2\theta \quad (1b)$$

where θ is the scan angle, β_0 and β_1 are the model parameters determined from the pitch maneuver data. The scan-angle dependent features of antenna brightness temperature for both quasi-vertical and quasi-horizontal polarization simulated from the antenna gain data are consistent with maneuver measurements. At nadir, the observed and simulated antenna brightness temperatures have a minimum at all QV channels and a maximum at all QH channels.

Scan angle dependent bias feature was also found in observations from NOAA legacy microwave sounding instruments. Sounders et al found that scan angle dependent bias existed in AMSU-B instrument during the thermal-vacuum test. They found that the bias is polarization dependent and is larger in nadir than those in scan edge (Sounders et al., 1995). By study the pitch-over observations from NOAA-14 MSU instrument, Kleespies also found that there is a marked asymmetry in the nominal Earth scene, and the characteristics of the asymmetry differ for the different polarizations. The vertically polarized channels display maximum difference from the space look near the nominal nadir position, while the horizontally polarized channels tend to have a maximum in the lower scan positions and a minimum in the higher scan positions (Kleespies, 2007). In the follow on study, Kleespies pointed out that the possible root cause of the scan dependent bias observed in pitch-over observations are contamination from Earth side-lobe and the thermal emission from the polarized scan mirror (Kleespies, 2011).

Study on F16-SSMIS instrument shows that thermal radiation from antenna reflector can be a major cause of calibration bias (Kunkee et al., 2008; Yan and Weng, 2009). For the spaceborne microwave sounding instruments, the antenna reflector is required to be

designed with a reflectivity of larger than 0.999. But the study on SSMIS calibration shows that the SIOx coating on the reflector surface may result in reduced reflectivity and consequently significant emission (Bell et al., 2006). The reflection coefficient for a specimen of the reflector material can be measured with a network analyzer. However, if the reflection coefficient is close to one, it becomes difficult, if not impossible, to achieve the measurement accuracy from the analyzer (Skou, 1997).

The root cause of the scan angle dependent bias observed in microwave sounding instrument TDR products is kept unknown for many years. In this paper, based on the study from different researchers on legacy NOAA MSU and AMSU instruments, and the analysis for on-orbit pitch over observations from the newest SNPP ATMS instrument, a theoretical model was established to explained the major root cause of scan angle dependent bias observed in NOAA microwave sounding instruments. This model is built based on the assumption that the polarized scan mirror plays a major role for the observed bias. A retrieval algorithm is then developed to get antenna reflector emissivity from ATMS cold space scan measurements during NPP satellite pitch-over operation. In Section II, a general reflector emission model is introduced. Section III is devoted for the model applied for pitch-over observations, the emissivity retrieval model and its impacts to calibration accuracy were described in section IV. The summary and discussions on the retrieval products and their possible applications will be given in Section V.

II. Antenna Reflection and Transmission Model

2.1 Characteristics of ATMS Antenna Reflector

ATMS has two receiving antennas, with one receiving antenna serving for channels 1-15 with frequencies below 60 GHz and a separate receiving antenna for channels 16-22 with

frequencies above 60 GHz. As shown in Fig. 1a, the antennas consist of a plane reflector mounted on a scan axis at a 45° tilt angle so that radiation is reflected from a direction perpendicular to the scan axis into a direction along the scan axis (i.e., a 90° reflection). With the scan axis oriented in the along-track direction, this results in a cross-track scan pattern. The reflected radiation is focused by a stationary parabolic reflector onto a dichroic plate (polarizing grid), and then either reflected to or passed through to a feedhorn. Each aperture/reflector serves two frequency bands for a total of four bands.

Due to the coating material used, the rotating plane reflector is not lossless and has its own thermal emission. According to Niels Skou's equation (Skou, 1997), the emissivity of a good conducting surface, viewed at normal incidence, is

$$\varepsilon_N = \frac{1}{15}\sqrt{\frac{f}{\sigma \cdot 10^7}}$$

where f is the receiver microwave frequency and σ is the conductivity of the reflecting surface. This equation should be valid for perfectly smooth and pure bulk conductive materials. For example, for bulk gold (σ=4.10E7) the equation gives 0.0014 at 183 GHz and 0.0005 at 23.8 GHz. The actual emissivity of real reflector surfaces is invariably greater than the computed theoretical value, due primarily to surface roughness and impurities. The ATMS flight reflector is made of Beryllium with a nominally 0.6 micron gold plating layer, on a Nickel interfacing layer. Since the gold plating thickness is comparable to the skin depth, and is likely to have extreme microscopic granularity and roughness, it is not unexpected that the emissivity would greatly exceed the values computed from the Skou's equation.

2.2 Mueller Matrices for Antenna Reflection and Transmission at 45 Incident Angle

As stated before, when the rotating flat reflector of ATMS become polarized, to evaluate its impact on reflected radiation, a full polarized physical model for antenna reflection is need to be established at first. Figure 1b shows how the scene radiation is reflected by the scan mirror. E_{sv}- E_{sh} is incident plane, by which the instrument polarization is defined as E-field perpendicular to the plane for H-pol and parallel to the plane for V-pol. E_{Rv}- E_{Rh} is the reflector scattering plane, by which the reflection polarization is defined as E-field perpendicular to the plane for H-pol and parallel to the plane for V-pol. Taking the scattering plane as reference, for a homogeneous bulk-material reflector, the Mueller matrices for reflection (M_R) and transmission (M_T) at an incidence angle of 45 degree can be expressed as (Dennis Goldstein, 2013):

$$M_R = \frac{1-sin2\theta_r}{(1+sin2\theta_r)^2}\begin{bmatrix} 1 & sin2\theta_r & 0 & 0 \\ sin2\theta_r & 1 & 0 & 0 \\ 0 & 0 & -cos2\theta_r & 0 \\ 0 & 0 & 0 & -cos2\theta_r \end{bmatrix} \quad (2a)$$

$$M_T = \frac{2sin2\theta_r}{(1+sin2\theta_r)^2}\begin{bmatrix} \frac{1+sin2\theta_r}{2}+1 & \frac{1+sin2\theta_r}{2}-1 & 0 & 0 \\ \frac{1+sin2\theta_r}{2}-1 & \frac{1+sin2\theta_r}{2}+1 & 0 & 0 \\ 0 & 0 & \sqrt{2}(cos\theta_r+sin\theta_r) & 0 \\ 0 & 0 & 0 & \sqrt{2}(cos\theta_r+sin\theta_r) \end{bmatrix} \quad (2b)$$

where θ_r is the refractive angle which is related to the incident angle through Snell's law, and the value of θ_r is close to zero for a metal.

When the ATMS antenna reflector scans to cold space or a blackbody target, the incident radiation is unpolarized and can be expressed in a Stokes vector as:

$$S = I_0\begin{bmatrix} 1 \\ 0 \\ 0 \\ 0 \end{bmatrix} \quad (3)$$

where I_0 is the radiance intensity. From (2a) and (2b), the reflected and transmitted Stokes components can be derived by multiplying (3) as

$$S_R = I_0 \frac{1-sin2\theta_r}{(1+\sin 2\theta_r)^2} \begin{bmatrix} 1 \\ sin2\theta_r \\ 0 \\ 0 \end{bmatrix} \tag{4a}$$

and

$$S_T = I_0 \frac{2sin2\theta_r}{(1+\sin 2\theta_r)^2} \begin{bmatrix} \frac{1}{2}(1+sin2\theta_r)+1 \\ \frac{1}{2}(1+sin2\theta_r)-1 \\ 0 \\ 0 \end{bmatrix} \tag{4b}$$

Here, subscript R and T stand for reflection and transmission of incident wave. Note that the sum of the reflected intensity and the transmitted intensity is equal to the incident intensity

$$S = S_R + S_T,$$

which is required from the principle of the conservation of energy. It is also interesting to note that after reflection, the incident unpolarized wave can become polarized, depending on the angle. It should be noted that in this context, polarization direction is defined in scattering plane: vertical polarization means E field parallel to scattering plane and horizontal polarization means E field perpendicular to scattering plane. For a reflection problem we are studying, it is more convenient to convert the reflected and transmitted vector in (4a) and (4b) to a modified Stokes vector as such:

$$S_R = \begin{bmatrix} S_{RV} \\ S_{RH} \\ S_{R3} \\ S_{R4} \end{bmatrix} = \frac{I_0}{2} \frac{1-sin2\theta_r}{(1+\sin 2\theta_r)^2} \begin{bmatrix} 1-sin2\theta_r \\ 1+sin2\theta_r \\ 0 \\ 0 \end{bmatrix} \tag{5a}$$

$$S_T = \begin{bmatrix} S_{TV} \\ S_{TH} \\ S_{T3} \\ S_{T4} \end{bmatrix} = \frac{I_0}{2} \frac{2sin2\theta_r}{(1+\sin 2\theta_r)^2} \begin{bmatrix} 2 \\ 1+sin2\theta_r \\ 0 \\ 0 \end{bmatrix} \quad (5b)$$

From (5a) and (5b), the horizontal and vertical amplitude reflection coefficients of antenna reflector can be expressed as:

$$r_h = \frac{1-sin2\theta_r}{1+sin2\theta_r}, r_v = \frac{(1-sin2\theta_r)^2}{(1+sin2\theta_r)^2} \quad (6a)$$

Similarly, we can get the transmission coefficients:

$$t_h = \frac{2sin2\theta_r}{(1+sin2\theta_r)}, t_v = \frac{4sin2\theta_r}{(1+sin2\theta_r)^2} \quad (6b)$$

From (6a) and (6b) we can see that:

$$r_h + t_h = 1, r_v + t_v = 1$$

A corresponding relation exists between polarization reflection coefficients:

$$r_h^2 = r_v \quad (7)$$

Note that the above relationship is true only at an incident angle of 45^o. Later, we will show that the relationship expressed in (7) will be very useful for determination of antenna emissivity or reflectivity.

III. ATMS Antenna Reflection Model for Pitch-over Observations

As descripted in previous section, it is very difficult to measure the ATMS antenna reflectivity from the ground tests. In this section, we prove that ATMS pitch-over observations can be used to quantify the antenna loss. When the reflector scans to an angle of θ relative to the feed horn orientation, the received antenna brightness temperature is a combination of the vertical and horizontal components (Weng et al.,

2013). Thus, the resulting signals reflected off the antenna can be expressed in the Stokes vector (Akira Ishimaru, 1990):

$$R_Q = \begin{bmatrix} R_{Qv} \\ R_{Qh} \\ R_{Q3} \\ R_{Q4} \end{bmatrix} = \begin{bmatrix} cos^2\theta & sin^2\theta & \frac{1}{2}sin2\theta & 0 \\ sin^2\theta & cos^2\theta & -\frac{1}{2}sin2\theta & 0 \\ -sin2\theta & sin2\theta & cos2\theta & 0 \\ 0 & 0 & 0 & 1 \end{bmatrix} \times (S_R + S_T) \quad (8)$$

Where S_R is the cold space radiation reflected by antenna reflector, S_T is thermal radiation from reflector. Their polarization state is defined in incident plane (scan plane). By applying the relationship between V and H reflectivity given in equation 7, S_R can be expressed as

$$S_R = R_S \frac{1-sin2\theta_r}{(1+\sin 2\theta_r)^2} \begin{bmatrix} 1+sin2\theta_r \\ 1-sin2\theta_r \\ 0 \\ 0 \end{bmatrix} = \begin{bmatrix} r_h R_S \\ r_h^2 R_S \\ 0 \\ 0 \end{bmatrix} \quad (9a)$$

and similarly S_T can be expressed as:

$$S_T = R_{rfl} \frac{2sin2\theta_r}{(1+\sin 2\theta_r)^2} \begin{bmatrix} 1+sin2\theta_r \\ 2 \\ 0 \\ 0 \end{bmatrix} = \begin{bmatrix} (1-r_h)R_{rfl} \\ (1-r_h^2)R_{rfl} \\ 0 \\ 0 \end{bmatrix} \quad (9b)$$

In equation 9, R_s is scene radiance and R_{rfl} is thermal radiance from antenna reflector itself. It needs be noted that to derive equation (8) and (9), the reference incident plane by which the polarization direction is defined is different. As shown in figure 1b, for ATMS observations, the incident plane is formed by beam direction and normal direction of local plane in earth surface ($E_{sv}Z$ plane in the figure). While for radiation reached in front

of the antenna reflector, the incident plane is formed by beam direction and the normal direction of antenna plane ($E_{Rv}Z_r$ plane in the figure). Since the two planes are perpendicular with each other, the V and H direction in these two planes are opposite.

Substituting S_R and S_T in (9) into (8) leads to the vector expression of radiation leave off reflector surface:

$$\begin{bmatrix} R_{Qv} \\ R_{Qh} \\ R_{Q3} \\ R_{Q4} \end{bmatrix} = \begin{bmatrix} R_s + e_h\left(R_{rfl} - R_s\right) + [(R_{rfl} - R_s)(e_v - e_h)]sin^2\theta \\ R_s + e_h\left(R_{rfl} - R_s\right) + [(R_{rfl} - R_s)(e_v - e_h)]cos^2\theta \\ \left(R_{rfl} - R_s\right) \cdot e_h \cdot (1 - e_h) \cdot sin2\theta \\ 0 \end{bmatrix} \quad (10)$$

In equation above, $e_h = 1 - r_h$ and $e_v = 1 - r_v$ are reflector emissivity at H and V polarization. $R_s = R_c$ when reflector scans cold space and $R_s = R_w$ when it scans to calibration blackbody target. Note that the QV/QH expressions derived here are actually consistent with those in equation 1, in which the model parameters β_0 and β_1 are expressed as functions of emissivity and physical temperature of reflector:

$$\beta_0 = e_h\left(R_{rfl} - R_s\right)$$

$$\beta_1 = (R_{rfl} - R_s)(e_v - e_h)$$

Equation (10) provides a physical model for simulating pitch over observations obtained through a polarized antenna reflector. It can be seen that when a non-lossless plane reflector is used to scan the scene, a uniform unpolarized radiation can be changed to polarized and expressed as a function of antenna reflectivity, reflector physical temperature, scene temperature, and scan angle. Figure 2 shows the simulated radiation in brightness temperature under different reflector temperature and reflectivity conditions. For Quasi-V channels, it is a square of the sinusoidal curve and for Quasi-H channels it follows a cosine curve. It can be seen that the impact of reflector thermal radiation can

become significant when the scene radiation equals cosmic background, which is the case for cold space view in ATMS scan cycle. For example, if the reflector reflectivity is only 0.994, then the cold target brightness temperature being used in calibration is not 2.73K deep space brightness temperature anymore, the thermal emission of reflector with a magnitude as large as 4.5K should be considered.

IV. Antenna Emission Estimated from Pitch-over Observations

4.1 Antenna Emissivity Retrieval Model

In normal observations, ATMS continually scans the Earth scene, cold space and warm load calibration target. During the pitch-over maneuver, the instrument turns to scan the un-polarized cold-space instead of the Earth scene at each of 96 scan positions. Given θ_s, θ_c, and θ_w are the scan angle for 'earth scene', cold space and warm load respectively, according to (10), the incident radiation from "earth scene" is:

$$R_{Qv}^{s} = R_{rfl} + r_h\left(R_c - R_{rfl}\right) + [(R_c - R_{rfl})(r_h^2 - r_h)]sin^2\theta_s \quad (11a)$$

$$R_{Qh}^{s} = R_{rfl} + r_h\left(R_c - R_{rfl}\right) + [(R_c - R_{rfl})(r_h^2 - r_h)]cos^2\theta_s \quad (11b)$$

Similarly, for cold space and warm load views, we have:

$$R_{Qv}^{c} = R_{rfl} + r_h\left(R_c - R_{rfl}\right) + [(R_c - R_{rfl})(r_h^2 - r_h)]sin^2\theta_c \quad (11c)$$

$$R_{Qh}^{c} = R_{rfl} + r_h\left(R_c - R_{rfl}\right) + [(R_c - R_{rfl})(r_h^2 - r_h)]cos^2\theta_c \quad (11d)$$

and

$$R_{Qv}^{w} = R_{rfl} + r_h\left(R_w - R_{rfl}\right) + [(R_w - R_{rfl})(r_h^2 - r_h)]sin^2\theta_w \quad (11e)$$

$$R_{Qh}^{w} = R_{rfl} + r_h\left(R_w - R_{rfl}\right) + [(R_w - R_{rfl})(r_h^2 - r_h)]cos^2\theta_w \quad (11f)$$

Assuming C_s, C_c, and C_w are the corresponding receiver output counts for scene, cold space and warm load respectively, and $\delta = \frac{C_s - C_c}{C_w - C_c}$. By applying the two-point calibration equation for Quasi-V channels, we can derive

$$\frac{R_{QV}^S - R_{QV}^C}{R_{QV}^W - R_{QV}^C} = \delta \qquad (12)$$

Substitute equation (11) into (12), the antenna emissivity at 45^0 angle (w.r.t scattering plane) for ATMS quasi-vertical channels can be solved as:

$$\varepsilon_h = \frac{\delta(R_w - R_c)}{\delta[(R_w - R_{rfl})sin^2\theta_w - (R_c - R_{rfl})sin^2\theta_c] - (R_c - R_{rfl})(sin^2\theta_s - sin^2\theta_c)} \qquad (13a)$$

Note that for Quasi-H channels, follows from equation 7, the antenna emissivity should be calculated as

$$\varepsilon_v = 1 - (1 - \varepsilon_h)^2 \qquad (13b)$$

Since ε_V and ε_h are much less than 1, it follows that $\varepsilon_V = 2\varepsilon_h$

By deriving equation (13), it is proved that the antenna emissivity can be accurately determined from space scan measurements by using two-point calibration equation without considering receiver nonlinearity. Given the facts that the antenna emissivity is a small number usually less than 0.01, to reach a high accuracy of measurement, a well known uniform scene with temperature much lower than the physical temperature of reflector is required, which is only can be achieved through deep space scan.

4.2 Reflector Emissivity Spectrum

On February 20, 2012, the Suomi NPP satellite made its pitch-over maneuver. The spacecraft is pitched completely off the Earth to enable ATMS to acquire full scans of deep space. During about 18-minute pitch-over maneuver, ATMS continually scans over

cold space across its 96 field of views (FOVs). These data sets are collected from homogenous, unpolarized cold space. As shown Fig. 3, SNPP satellite platform pitch maneuver was carried out with a speed of 0.18^{o}/s. The pitch angle reached maximum of 179.4^{o} during the process. The cold calibration count profile is also changing with the pitch angle, this can be explained by the earth contamination through a side lobe. As pitch angle increases, the earth contamination to cold space view decreases. To reduce the impacts of earth contamination in deep space view, only ±25 scan lines at the maximum pitch angle were selected for retrievals of antenna emissivity. Figure 4 shows the averaged scene counts for cold space view and the standard deviation at each of 96 FOVs. These count observations closely follow the sinusoidal and cosine rule described by (1) although the count standard deviation is about 4 which is related to the instrument noise signal. In addition, there is an asymmetry feature in the space view observations which may be related to polarization angle twist and side-lobe effect. To get the clean deep space scan observations, near-field radiation models in (1) are used to fit the mean space view observations, as shown in Fig. 4b. The mean space observation fitted from (1) is then used to retrieve the antenna emissivity.

Based on the pitch-over observation datasets described above, the ATMS reflector emissivity is determined by using model expressed in Eq. (13) and is shown in Fig. 5. It should be noted that since the reflector emissivity is defined w.r.t reflector scattering plane, which is different from the scan plane in which the instrument polarization is defined, the retrieved H-pol emissivity should be used for QV channels and V-pol emissivity for QH channels. The retrieved emissivity at each band is listed in Table 2. In general, the spectral emissivity is in a range of 0.0026 to 0.0063. The emissivity at V-

polarization is larger than that at H-polarization (figure is omitted). Compare to the emissivity computed from Skou's equation, the retrieved ATMS emissivity is much larger, with a factor 6 higher for 23.8GHz and 5 higher for 183GHz. Since the reflector emission can not be ignored, it needs to be evaluated and corrected in calibration process.

4.3 Impact of Antenna Emissivity on the Earth Observations

ATMS is an instrument with less than 1K (0.75K for V band) calibration error is required for NWP applications. It is important for user to know the impact of antenna emissivity on calibration accuracy of the data products. Since the radiation from cold space, warm load and the Earth scene are all collected through the polarized flat reflector, the impact of antenna emissivity on Earth scene includes two parts: 1) extra error will be introduced into calibration equation due to uncorrected antenna emissivity on calibration target, and 2) the calibrated earth scene brightness temperature will be contaminated directly by the reflector thermal radiation if not corrected. In this paper, we mainly focused on assessing the impact of antenna emissivity on calibration accuracy. Its impact on observed earth scene brightness temperature will be discussed in future work.

To evaluate the impact of antenna emissivity on calibration accuracy, we need to start from calibration equation of ATMS instrument:

$$R_s = R_{bI} + Q_b \tag{14}$$

In equation above, R_{bI} is linear part of calibrated scene temperature, and can be computed from calibration targets by two-point calibration equation as:

$$R_{bI} = \delta \cdot (R_w - R_c) + R_c \tag{15}$$

where R_w and R_c are radiance for warm load and 2.7K cold space, $\delta = \frac{C_s - C_c}{C_w - C_c}$.

In equation (14), Q_b is nonlinear part of calibrated scene temperature, which can be expressed as function of maximum nonlinearity Q_{max} as below:

$$Q_b = Q_{max} \cdot [4 \cdot (\delta - 0.5)^2 - 1] \tag{16}$$

$$Q_{max} = \frac{1}{4} \cdot \mu \cdot (R_w - R_c)^2$$

where μ is nonlinearity parameter and can be derived from TVAC test data.

The error model for calibrated scene temperature due to antenna emissivity correction can be built from equations (14) ~ (16) as:

$$\Delta R_s = \delta \cdot (\Delta R_w - \Delta R_c) + \Delta R_c + \frac{1}{4} \cdot \Delta\mu \cdot (\Delta R_w - \Delta R_c)^2 \cdot [4 \cdot (\delta - 0.5)^2 - 1] \tag{17}$$

It is known from equation (17) that the calibration errors arise from antenna emission are depend on three terms: radiance error in cold space and warm load, and error in nonlinearity parameters. From Equation (11), explicit form of radiance error in calibration target can be derived as:

For Quasi V channels:

$$\Delta Rx = \varepsilon_h (R_{rfl} - R_x) + (R_{rfl} - R_x) \cdot (\varepsilon_v - \varepsilon_h) \cdot sin^2\theta_x \tag{18a}$$

For Quasi H channels:

$$\Delta Rx = \varepsilon_h (R_{rfl} - R_x) + (R_{rfl} - R_x) \cdot (\varepsilon_v - \varepsilon_h) \cdot cos^2\theta_x \tag{18b}$$

In equation (18), ΔRx can be ΔR_c or ΔR_w.

By using equation (17), the impact of antenna emissivity to calibration error then can be assessed. Figure 6 shows the scene temperature dependent calibration error at K,V W and G band of ATMS. To derive the simulation results, temperatures of reflector and warm

load are retrieved from on-orbit PRT measurements of ATMS, nonlinearity parameters are derived from SNPP ATMS TVAC test under middle receiver temperature conditions.

It can be seen that the calibration error decrease with increased scene temperature. For K band, calibration error can be as large as 1.5K at 2.7K space view, and decrease to -0.1K at 300K Earth scene observation. Due to the different reflectivity characteristic at ATMS channels, the magnitude of calibration error at different channel is also different. W band was observed with the largest error, which can be explained by the relatively larger emissivity in this channel.

V. Conclusion and Discussion

ATMS antenna reflector can emit the radiation due to the coating material and surface roughness and have an impact on calibration accuracy. Its cross-track rotation can complicate its emission problem by changing the polarization state of incident wave.

When reflector reflectivity is approach to 1, it is very difficult to be measured in ground test. Since there are no improvements have been made for JPSS-1 ATMS antenna, Pitch over maneuver operation is very critical for the measurement of the reflector emissivity spectrum in space, it provide a very unique dataset from which the reflector emissivity can be retrieved from the deep space observations with very high accuracy, which is not achievable in ground test.

In this paper, we develop a technique to estimate the ATMS plane reflector emission for frequency ranging from K to W bands.

Using the Mueller matrix of reflection and transmission at 45^{o} angle for a bulk-material reflector, we derived a full vector expression for reflected radiation for non-lossless,

polarized rotating reflector. The physical model is then applied to the two-point calibration equation and the antenna emissivity can be derived from the pitch-over observations. The reflector emissivity spectrum ranges from 0.002 to 0.006 from K to G bands.

Error model are also developed to assess the impacts of antenna emissivity to calibration. Results show that the calibration error can be as large as 2.5K for space view at channel 16. The error is scene dependent and different for different channel of ATMS due to the nonlinearity characteristic at each channel. For unpolarized channels the scan dependent feature of TDR error is dominated by sine square term at quasi-V channels and cosine square term in quasi-H channels. For polarized window channels, the impacts of antenna emissivity to observed scene brightness temperature are complicated by the rotation of polarization state, which will be studied in our future work.

References

A. Ishimaru, 1991: Electromagnetic Wave Propagation, Radiation, and Scattering, 637 pages, Prentice Hall, New Jersey

B. Yan and F. Weng, 2009: Assessments of F16 Special Sensor Microwave Imager and Sounder Antenna Temperatures at Lower Atmospheric Sounding Channels, Advances in Meteorology , doi:10.1155/2009/420985

D. B. Kunkee, S. D. Swadley, G. A. Poe, Y. Hong, and M. F. Werner, 2008, Special Sensor Microwave Imager Sounder (SSMIS) Radiometric Calibration Anomalies—Part I: Identification and Characterization, IEEE TRANSACTIONS ON GEOSCIENCE AND REMOTE SENSING, VOL. 46, NO. 4, PP. 1017-1033

F. Weng, H. Yang, and X. Zou, 2013: On Convertibility from Antenna to Sensor Brightness Temperature for ATMS, IEEE GEOSCIENCE AND REMOTE SENSING LETTERS, VOL. 10, NO. 4, PP.771-775

N. Skou, 1997: Measurement of Small Antenna Reflector Losses for Radiometer Calibration Budget, IEEE TRANSACTIONS ON GEOSCIENCE AND REMOTE SENSING, VOL. 35, NO. 4, JULY 1997, PP. 967-971

W. Bell,A Preprocessor for SSMIS Radiances Scientific Description, Met Office, UK. Doc ID : NWPSAF-MO-UD-014 Version : 1.0

Dennis Goldstein, 2013, “Polarized Light”, second edition, Marcel Dekker, Inc

Roger W. Saunders, Timothy **J.** Hewison, Stephen **J.** Stringer, and Nigel C. Atkinson, 1995, The Radiometric Characterization of AMSU-/B, IEEE TRANSACTIONS ON MICROWAVE THEORY AND TECHNIQUES, VOL. 43, NO. 4, PP. 760-771

Thomas J. Kleespies, Renee Smith-Dearring, Jonathan Woodward, James Shepherd, Carl Gliniak, William Chadwick, James Walters, and Dong Han, 2007, Evaluation of Scan Asymmetry in the NOAA-14 Microwave Sounding Unit by a Pitch Maneuver, IEEE GEOSCIENCE AND REMOTE SENSING LETTERS, VOL. 4, NO. 4, PP. 621-623

Thomas J. Kleespies, 2011, Recharacterization of the Microwave Sounding Unit Cross-Track Asymmetry During a Spacecraft Tumble, Geoscience and Remote Sensing Letters, IEEE 8.2 (2011): 230-232

Table 1 SNPP ATMS Channel Characteristics

Table 2 Retrieved mean emissivity value ATMS K, V, W and G bands

Figure 1a. Schematic diagram of ATMS antenna subsystem. The top portion shows the antenna subsystem for K/Ka and V bands whereas the lower portion is for W/G bands.

Figure 1b. Sketch plot for polarization direction definition by taken scan plane and reflection plane as reference frame respectively.

Figure 2. Simulated cold space observations from antenna reflection for quasi-H (left) and quasi-V channels (right). Scene temperature is sent to 2.73K, reflector physical temperature is set to 300K. red, blue and black line is corresponding to antenna reflectivity equals to 0.992,0.996 and 0.998 respectively.

Figure 3. ATMS pitch-over observations at channel 1. From left to right is scene counts, profiles for pitch angle, nadir scene counts, cold calibration counts at 97^{th} FOV

Figure 4. Mean (blank line) and standard deviation (bars in dark gray) of space scan at each of 96 FOVs at left, and model simulated (black line) and real observed receiver output space view counts (square points) at right. Upper panel is for channel 1 (smile shape) and lower panel is for channel 3 (frown shape)

Figure 5. Retrieved reflector emissivity for ATMS K, V, W and G bands

Figure 6. Scene temperature dependent calibration error at K,V, W and G band of ATMS from error model

Table 1. SNPP ATMS Channel Characteristics

Ch	Channel Central Freq.(MHz)	Polarization	Bandwidth Max. (MHz)	Frequency Stability (MHz)	Calibration Accuracy (K)	NEΔT (K)	3-dB Bandwidth (deg)
1	23800	QV	270	10	1.0	0.5	5.2
2	31400	QV	180	10	1.0	0.6	5.2
3	50300	QH	180	10	0.75	0.7	2.2
4	51760	QH	400	5	0.75	0.5	2.2
5	52800	QH	400	5	0.75	0.5	2.2
6	53596±115	QH	170	5	0.75	0.5	2.2
7	54400	QH	400	5	0.75	0.5	2.2
8	54940	QH	400	10	0.75	0.5	2.2
9	55500	QH	330	10	0.75	0.5	2.2
10	57290.344(f_o)	QH	330	0.5	0.75	0.75	2.2
11	f_o ± 217	QH	78	0.5	0.75	1.0	2.2
12	f_o ±322.2±48	QH	36	1.2	0.75	1.0	2.2
13	f_o ±322.2±22	QH	16	1.6	0.75	1.5	2.2
14	f_o ±322.2±10	QH	8	0.5	0.75	2.2	2.2
15	f_o ±322.2±4.5	QH	3	0.5	0.75	3.6	2.2
16	88200	QV	2000	200	1.0	0.3	2.2
17	165500	QH	3000	200	1.0	0.6	1.1
18	183310±7000	QH	2000	30	1.0	0.8	1.1

19	183310±4500	QH	2000	30	1.0	0.8	1.1
20	183310±3000	QH	1000	30	1.0	0.8	1.1
21	183310±1800	QH	1000	30	1.0	0.8	1.1
22	183310±1000	QH	500	30	1.0	0.9	1.1

Table 2 Antenna Reflector Emissivity at ATMS K, V, W and G band

Bands Name	Reflector Emissivity
K	0.0026
V	0.0036
W	0.0043
G	0.0063

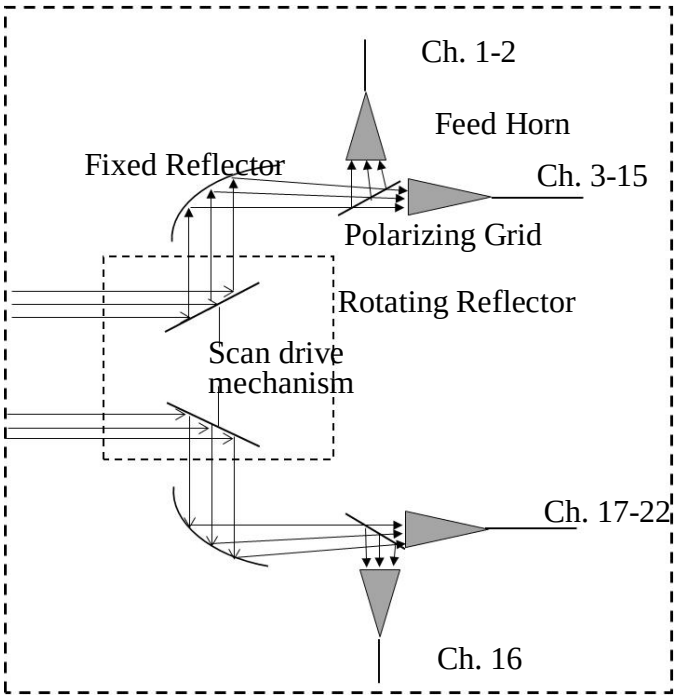

Figure 1a. Schematic diagram of ATMS antenna subsystem. The top portion shows the antenna subsystem for K/Ka and V bands whereas the lower portion is for W/G bands.

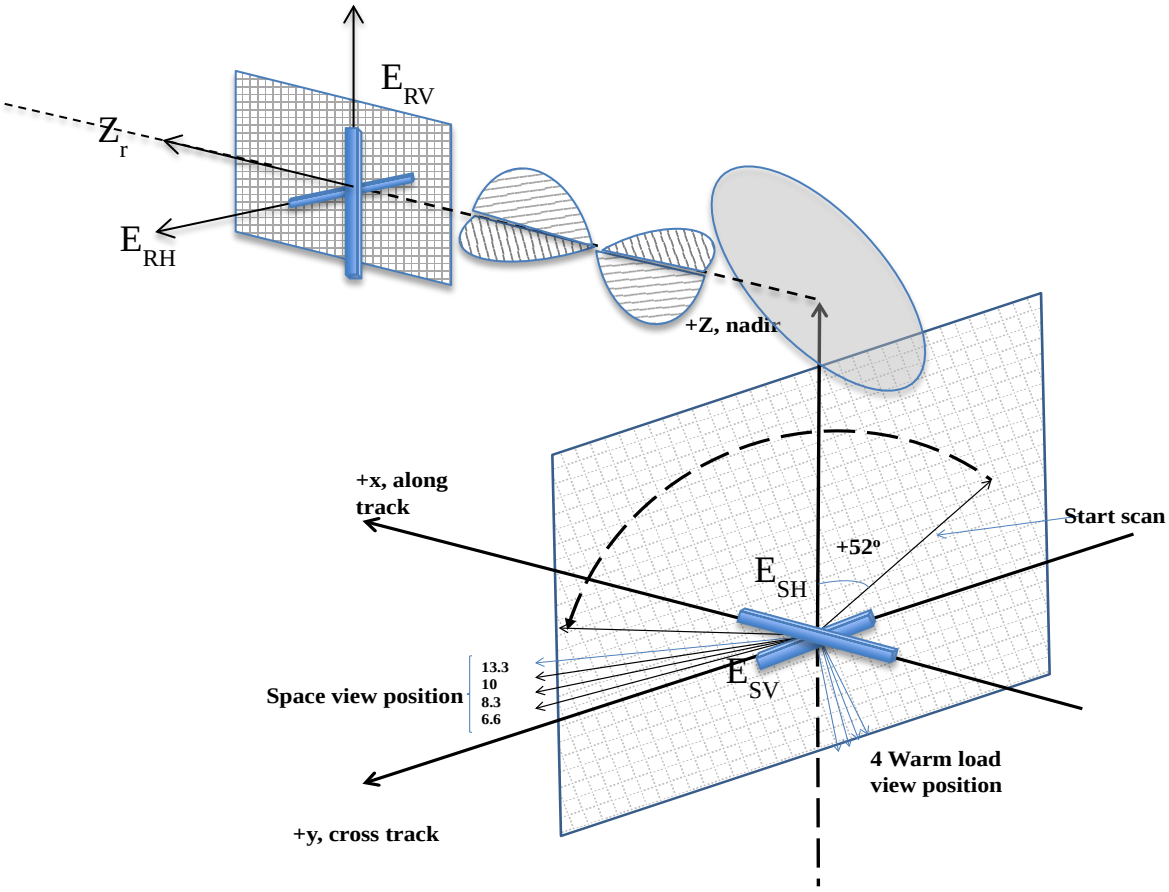

Figure 1b. Sketch plot for polarization direction definition by taken scan plane and reflection plane as reference frame respectively.

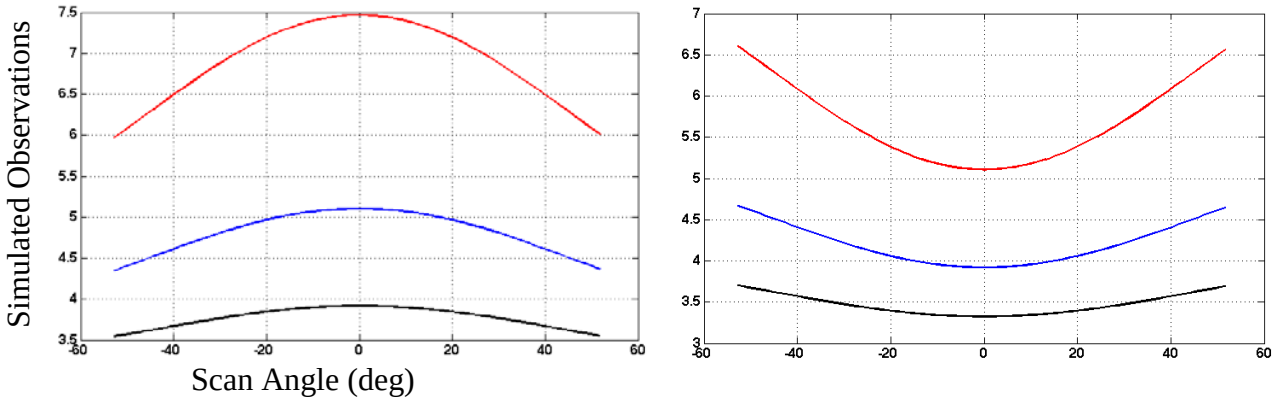

Figure 2 Simulated cold space observations for quasi-H (left) and quasi-V channels (right). Scene temperature is set to 2.73K, reflector physical temperature is set to 300K. red, blue and black line is corresponding to antenna reflectivity equals to 0.992,0.996 and 0.998 respectively.

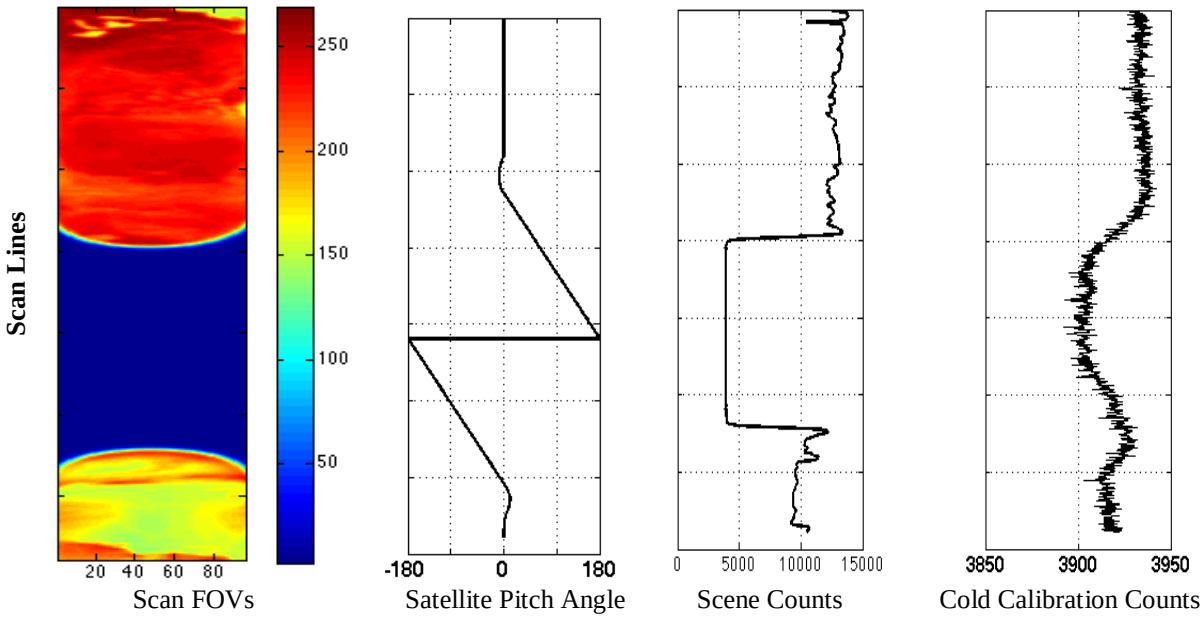

Figure 3. ATMS pitch-over observations at channel 1. From left to right is scene temperature, profiles for pitch angle, nadir scene counts and cold calibration counts at 97th FOV

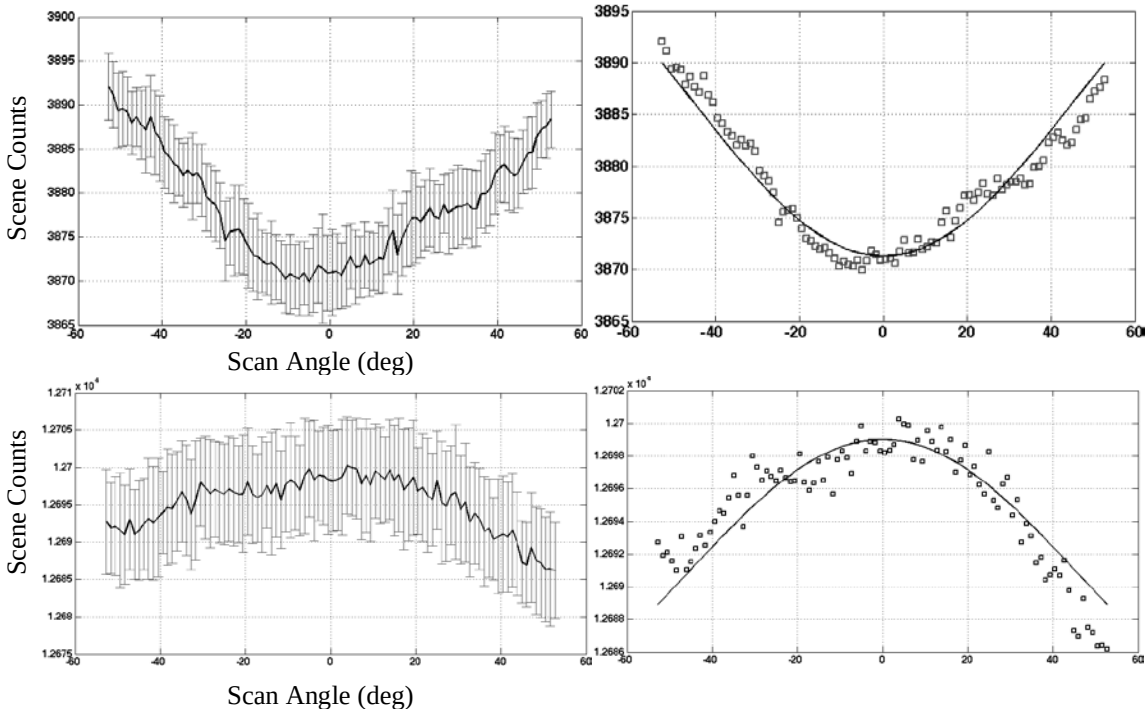

Figure 4. Mean (blank line) and standard deviation (bars in dark gray) of space scan at each of 96 FOVs at left, and model simulated (black line) and real observed receiver output space view counts (square points) at right. Upper panel is for channel 1 (smile shape) and lower panel is for channel 3 (frown shape)

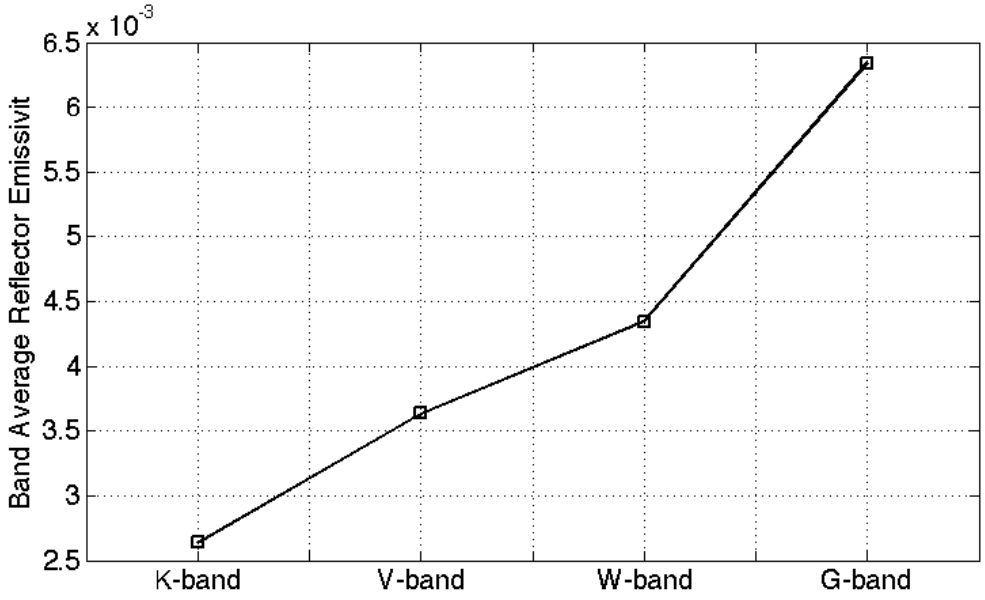

Figure 5 Band average reflector emissivity for ATMS K, V, W and G band

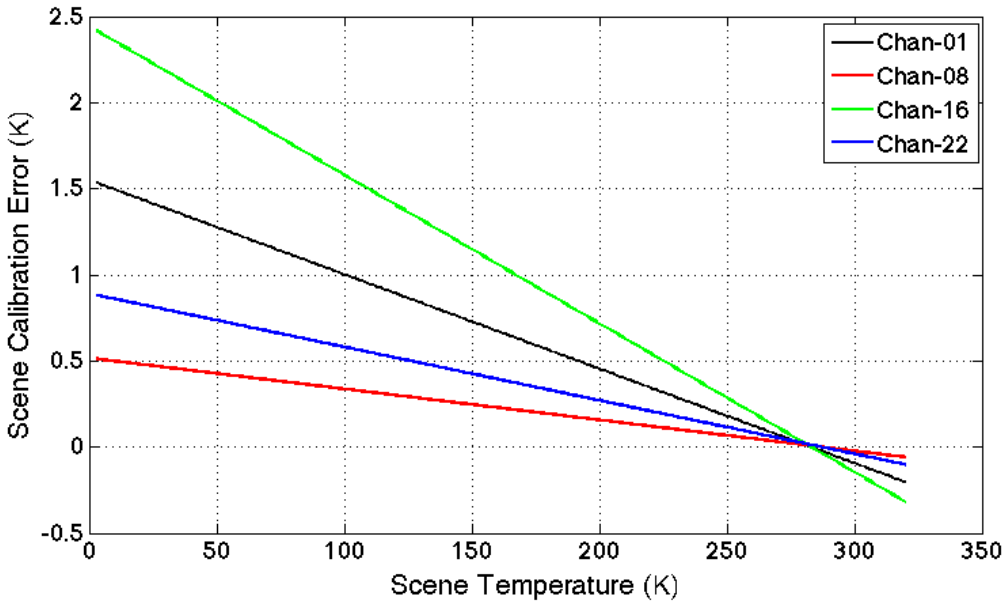

Figure 6. Scene temperature dependent calibration error at K,V W and G band of AMTS from error model. Temperatures of reflector and warm load are retrieved from on-orbit PRT measurements of ATMS, nonlinearity parameters are derived from SNPP ATMS TVAC test under middle receiver temperature conditions.